Weight-Constrained Reliability Allocation for All Electric Aircraft Powertrains

Jinghao Li, Yiwen Huang, Ran Li, *Member, IEEE,* Hao Hua, Fei Gao, *Member, IEEE,* Xiaoze Pei, Wentao Huang, *Member, IEEE,* Nengling Tai, *Member, IEEE*

***Abstract*—The shift towards electric aircraft poses significant challenges in balancing lightweight design and high reliability of powertrains. Typically, improving reliability requires redundancy, which adds weight, while lightweight designs often compromise reliability. In this paper, we propose a weight-constrained reliability allocation model for the powertrain design of electric aircraft. The relationship between reliability and weight for each component, including battery, inverter, and electric motor is analytically and linearly expressed using universal generating functions (UGF) and McCormick envelope technique. Our model considers variable operating conditions that impact component reliability, such as changes in core temperature caused by high-attitude and variable thrust power caused by wind speed and direction. Our approach enhances the overall performance of electric powertrains systems for aircraft. Using the " Spirit of Innovation " electric aircraft as a case study, the proposed method can improve the powertrain reliability from 0.9786 to 0.9870 through reasonable allocation without adding extra weight. Alternatively, it can reduce the weight by 3.1% without compromising the reliability of the powertrain.**

***Index Terms*—Electric aircraft, reliability allocation, two-stage optimization, weight constraints, actual operating conditions**

NOMENCLATURE

UGF	Universal generating functions
PMSM	Permanent magnet synchronous machine
Cost	the total cost
C_I	annualized system initial investment cost
$C_{O\&M}$	annualized system operation and maintenance cost
$R_s(A)$	the system reliability
A	the availability vector
C	the specific heat capacity
△T	temperature variation
P_D	power used by each component for heating
A_h	contact area between the component and the air
M	weight of the aircraft
V	the speed of the plane relative to the air
TN	the thrust of the aircraft
L	the lift of the aircraft
D	the drag of the aircraft
C_L	the lift coefficient
C_D	the drag coefficient
ρ	air density
P	aircraft power
S_a	projected area of the aircraft wing
α	the angle of attack of the aircraft
γ	the climb angle of the aircraft
$\prod R_i(m_i)$	the series system reliability
Ri	the reliability of ith subsystem
m_i	the mass *of ith* subsystem
M_s	the mass of system
u_{wind_acc}	uncertain variables of wind acceleration
U	Uncertain set
k	the current number of iterations
y_l	the solution of the subproblem after the lth iteration
u^*_l	the solution of the worst-case scenario after the lth iteration
k_i	the influence coefficient of each degree of the ith sub-system on the electric powertrain
$T_{i,s}$	the rated temperature of the ith sub-system
$\bar{T}_i$	the average temperature during actual operation
R_{Bat}	battery reliability
R_{Bat1}	battery voltage reliability
R_{Bat2}	battery capacity reliability
P_{cr}	the cruising power of the aircraft
R_g	the range of the aircraft
η	the efficiency of powertrain
ρ_0	the energy density of the used cell
ρ	the energy density of the battery pack

Jinghao Li, Yiwen Huang, Ran Li, Hao Hua, Wentao Huang and Nengling Tai are with the Key Laboratory of Control of Power Transmission and Conversion, Ministry of Education, Shanghai Jiao Tong University, Shanghai 200240, China(e-mail: ljh641670192@sjtu.edu.cn; hyw1998@sjtu.edu.cn; rl272@sjtu.edu.cn;huahao@sjtu.edu.cn;hwt8989@sjtu.edu.cn;nltai@sjtu.edu.cn). *(Corresponding author: Ran Li).* Yiwen Huang is co-first author.

Fei Gao is with the Department of Electrical Engineering, Shanghai Jiao Tong University, Shanghai 200240, China (e-mail: sjtugf@163.com).

Xiaoze Pei is with the Department of Electrical Engineering, The University of Bath, Bath BA2 7AY, U.K. (e-mail:X.Pei@bath.ac.uk)

I. INTRODUCTION

Electrically-powered transportation vehicles, such as electric aircraft, offer advantages including emission-free operation, low noise, high efficiency, and compactness [1]. Several studies have investigated electric powertrains for cars and ships [2]-[4], while others have focused on aircraft and helicopter propulsion systems [5]. Compared to other

transportation vehicles like cars and ships, aircraft operate in unique environments and have severe consequences in case of accidents. There have been reports of aircraft accidents caused by electrical equipment failure in 2008, 2010, and 2014 [6]. Therefore, the reliability of electric aircraft, particularly the reliability of their electric powertrains, is crucial for both economic and safety reasons.

However, there is a trade-off between weight and reliability in electric aircraft propulsion systems. For example, aircraft requires contingency reserves to guarantee reliability and considers factors such as weather conditions. These reserves, however, lead to a trade-off as they contribute to the aircraft's weight and increase energy consumption. It is also a common practice for terrestrial power systems to use redundancy for reliability enhancement. A methodology to determine a rational redundancy level of power system equipment was proposed in [7], which performed reliability and economic analyses of the equipment redundancy scheme. The design issue for the optimal number of redundant units in a triple-modular-redundancy system with redundant units was addressed in [8]. However, the critical challenge for all-electric aircraft is the limited range due to the low energy density of batteries. Typical electric aircraft have a range of 200-500 km, while their fossil-fuel counterparts can reach up to 1600 km [1]. Therefore, the redundancy-based reliability enhancement approach is not practical for the design of electric aircraft powertrains.

Another approach to improve reliability is reliability allocation. Reliability allocation refers to the distribution of system reliability indicators to subsystems, equipment, or components at different functional levels with the aim of minimizing the total cost under certain reliability constraints. Existing literature usually models it as an optimization problem, such as redundancy allocation [9], [10], [11], minimization of system cost subject to reliability constraint [12], maximization of system reliability under cost constraint [13], or system reliability optimization more generally [14], [15], [16]. The reliability allocation problem of electric aircraft was studied in [17] based on cost optimization, but the effect of the resulting weight changes on the system was not considered. Despite extensive research into diverse modelling and optimization techniques, weight considerations have been absent from the literature as far as we have reviewed.

It is a challenging task to incorporate weight into the reliability allocation model. First, the relationship between weight and reliability is not yet clear although a significant number of papers attempted to model the cost and reliability variations of powertrain components. Second, component reliability is dynamically affected by the aircraft's operating environment, with the flight profile affected by weather conditions such as temperature, altitude, wind speed and direction. The change in temperature and thrust power will break the optimal balance between weight and reliability.

Therefore, this paper proposes a two-stage reliability allocation method for electric powertrains that considers weight constraints. This paper's main innovations are as follows:

1)This paper investigate the balance between reliability and weight for the application of electric aircraft powertrain design. A novel reliability allocation model is proposed in which reliability replaces cost as the objective and weight replaces reliability as the constraint. The weight and reliability of subsystems are analytically expressed and embedded as constraints in the model using Monte Carlo sampling and envelope fitting.

2) Instead of a static design under nominal conditions, the proposed two-stage method considers the uncertain external environment of electric aircraft. The impact of attitude, temperature and uncertain wind speed and direction on component reliability and thrust power is considered.

The weight-constrained reliability allocation model proposed in this paper is a generic framework that can be used for the design and optimization of various types of electric aircraft powertrains. In this study, we focus on a single-seat electric aircraft with a power level of 400 kW and equipped with three engines, to demonstrate the effectiveness of our approach. Future research can build on this framework to include different materials such as cryogenic electric aircraft or different characteristics such as volume. The framework can also be expanded with more detailed aerodynamic models and advanced optimization solvers.

The rest of this paper is organized as follows: Section II presents the formulation of the proposed two-stage optimization model. Section III describes the modelling of subsystem weight and reliability function. Section IV presents a case study, and Section V concludes the paper.

II. Weight-Constrained Reliability Allocation Model

A. Problem Description

Reliability allocation involves assigning reliability targets to specific components or subsystems within a system to achieve an overall reliability target. This process involves identifying critical components or subsystems that contribute most to the system's reliability and allocating reliability requirements based on their contribution. It is widely used in the power industry to pursue cost-effective designs that meet reliability requirements.

(1)-(4) form a generic reliability allocation model with cost as the objective (1) and reliability as the constraints (2-3). Other constraints, such as power flow constraints and start/stop constraints, are also considered in the optimization process.

$$\text{Min } C = C_I + C_{O\&M} \tag{1}$$

Subject to

$$R_{obj} \le R_s(A) \tag{2}$$

$$A_{\min} \le A \le A_{\max} \tag{3}$$

$$other\ constrains \tag{4}$$

The reliability requisites of electric aircraft powertrains are commensurate with, or exceed, those of conventional aircraft systems. Typically encompassing energy storage devices such as batteries or supercapacitors, the powertrain generates thrust via motors that actuate propellers, bypass fans, or other

propulsion mechanisms. This investigation centers on a particular subset of electrified components, namely the lithium battery pack, power electronics, and motor, to validate the efficacy of the proposed reliability allocation model. It is pertinent to emphasize that the constructed framework is inherently adaptable and poised for future expansion to include a more comprehensive set of electric aircraft powertrain elements. For the scope of this research, the selected components serve to exemplify the capability of the proposed method in augmenting the reliability and weight optimization of all-electric aircraft powertrains. Section II's ensuing subsections delineate the construction of our bi-level optimization model, the articulation of subsystem weight and reliability functions, the characterization of ambiguous parameters, and the assessment of reliability in the presence of uncertainty.

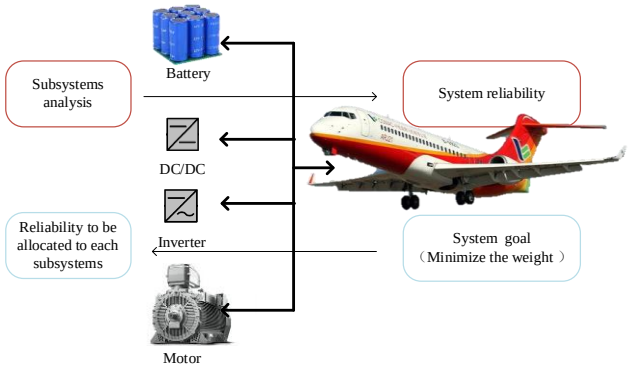

Fig. 1. Electric aircraft reliability allocation

As depicted in Fig.1, the reliability of electric powertrains is contingent on the reliability of individual sub-components, with the specific functional form being intimately tied to the powertrain's topology. The challenge resides in apportioning reliability to each constituent of the powertrain in a manner that optimizes reliability subject to weight constraints. This problem can also be framed as the minimization of the aggregate powertrain weight, concomitant with the preservation of a reliability threshold that surpasses predefined standards.

B. Rationale of two-stage Reliability Allocation for electric aircraft powertrain design

Reliability allocation is a crucial step in the design of electric aircraft powertrains. However, traditional reliability allocation methods often assume a constant operating temperature, which may not accurately reflect the actual operating conditions of the system. This can lead to significant deviations from the optimal solution in terms of reliability and cost. In reality, the reliability of subsystems in electric aircraft powertrains is affected by various factors such as operating conditions, wind speed/direction, and temperature. These factors have a significant impact on the system's reliability and thrust power. For example, changes in wind speed/direction can cause fluctuations in the load on the powertrain, leading to variations in temperature and reliability. Therefore, it is important to consider these factors in the reliability allocation process.

To address this issue, we propose a two-stage robust reliability allocation method that takes into account the actual operating conditions of the electric aircraft powertrain. In the first stage, we consider the standard temperature and environmental conditions to obtain an initial reliability allocation solution. In the second stage, we use a sensitivity analysis approach to adjust the initial solution based on the actual core temperature of components, which is closely related to the environmental temperature and component weight. Two-stage mutual iteration is performed to obtain the optimal reliability allocation. This two-stage approach allows for a more accurate and reliable allocation of system reliability, taking into account the effects of operating conditions, wind speed or direction, and temperature.

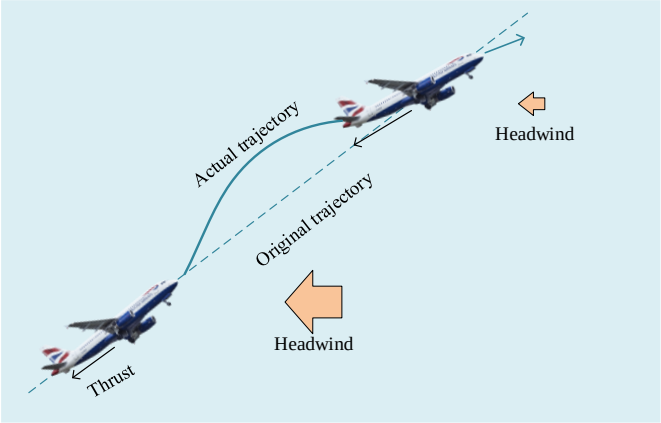

Fig.2 The actual flight profile of the aircraft

Fig.2 illustrates the scenario where the aircraft encounters headwinds during the climbing process, resulting in changes in the actual flight path due to the wind. Adopting different propulsion powers would lead to variations in the actual trajectory. The propulsion power affects the temperature changes in the electric powertrain. The temperature of the electric powertrains is not only affected by the power, but also by heat convection, which can be described by (5).

It relates the heat generation, weight, and temperature of the subsystem.

$$C m \triangle T = \int P_D \text{-} h A dt \tag{5}$$

C. Weight constraint reliability allocation Model

In this section, we present a modeling approach for aircraft dynamics during different stages of flight profiles, which generally include take-off, climb, cruise, and landing. Given the variations in pitch angle and lift/drag coefficients at each stage, we can derive the required thrust and navigation speed according to the forces acting on the aircraft, and subsequently determine the power required for each stage, as illustrated in Fig. 3 and described by (6)-(10). By incorporating these factors into the reliability allocation optimization model, we can obtain a more accurate and effective allocation strategy that accounts for the uncertainty and variability of flight conditions.

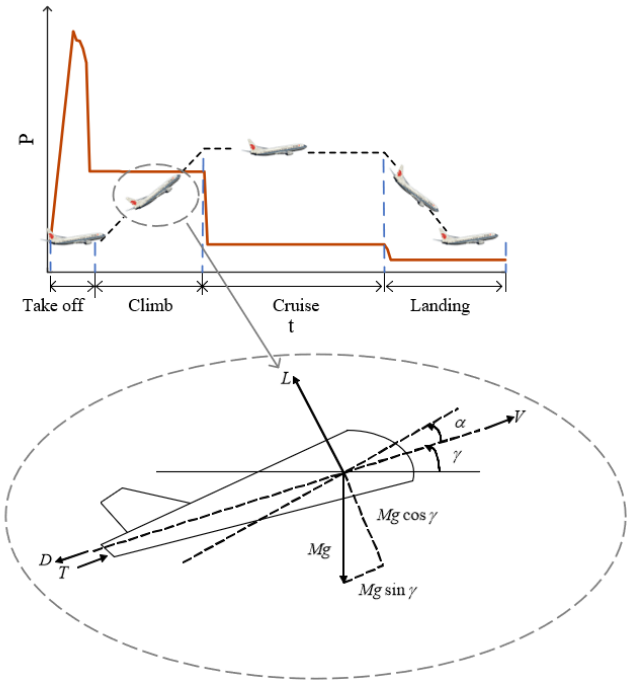

Fig. 3 The aircraft flight profile

$$M\dot{V} = TN\cos\alpha - D - Mg\sin\gamma \tag{6}$$

$$MV\dot{\gamma} = TN\sin\alpha + L - Mg\cos\gamma \tag{7}$$

$$L = \frac{1}{2}\rho V^2 S_a C_L \tag{8}$$

$$D = \frac{1}{2}\rho V^2 S_a C_D \tag{9}$$

$$P = TV \tag{10}$$

The objective of reliability allocation is to maximize the system reliability, as described by (11), subject to the constraints outlined in (12)-(14).

$$\max_m \prod R_i(m_i) \tag{11}$$

Subject to

$$R_{i,\min} < R_i < R_{i,\max} \tag{12}$$

$$m_{i,\min} < m_i < m_{i,\max} \tag{13}$$

$$\sum m_i = M_s \tag{14}$$

The above model is a nonlinear model that can be solved by conventional deterministic optimization methods after linearization. However, aircraft face many random factors during actual operation, and solutions obtained from deterministic optimization models often appear too risky, necessitating consideration for the effects of uncertainty in the models. Once the initial wind speed is determined, the wind speed can be determined by the acceleration of the wind. So in this study, the uncertainty set U was constructed by (15) to represent the fluctuation range of wind acceleration.

$$\mathrm{U}:=\left\{u_{wind\_acc}(t)\in[u_{LB},u_{UB}]\right. \tag{15}$$

where u_{wind_acc} are uncertain variables of wind acceleration introduced after considering uncertainty.

The objective of the two-stage robust optimization model proposed in this paper is to determine the optimal reliability allocation scheme that can withstand the worst-case scenario of uncertain variables within the set U, as expressed below.

$$\max_x\{\min_{y\in\Omega(x,u)}\max_{u\in U} c^T y\} \tag{16}$$

where the maximization of the outer layer is the first-stage problem and the optimization variables are *x*; the minimization of the inner layer is the second-stage problem and the optimization variables are *u* and *y*.

D. Solution method

To solve the two-stage robust optimization model, this paper employs the column constraint generation algorithm (C&CG). This algorithm decomposes the original problem into a master problem and a sub-problem, which are solved alternately to obtain the optimal solution of the original problem. Specifically, the decomposition of (16) results in a master problem in the following form:

$$\begin{cases} \max\limits_x \alpha, \\ s.t\ \alpha \ge c^T y_l \\ Ay_l \ge a \\ By_l = 0 \\ Cx + Dy_l \ge b \\ I_u y_l = u^*_l \\ \forall l \le k \end{cases} \tag{17}$$

where A、B、C、D、I_u are the coefficient matrix of the variables under the corresponding constraints, *a* ,*b* and *c* are constant series vectors.

The decomposed subproblem takes the form shown in (18). Due to the challenges in expressing the fluctuation of system reliability using power *P*, it is represented using temperature *T*. Additionally, after setting the initial temperature, the power of the previous moment can be uniquely determined by the temperature at each moment using (18). Therefore, the decision variable temperature *T* is used in place of power *P*.

$$\begin{aligned} &\min_{R\in\Omega(m,u)}\max_{u\in U}\Delta R(T) \\ &= \min_{R\in\Omega(m,u)}\max_{u\in U}\sum k_i(T_{i,s}-\overline{T}_i) \end{aligned} \tag{18}$$

The subproblem satisfies the constraints in the Appendix:

(A1) and (A2) describe the force balance between the two directions of the aircraft, while (A3) and (A4) represent the relationship between the speed and acceleration of the aircraft and the wind, respectively. (A5) and (A6) describe the lift and drag of the aircraft, respectively. (A7) represents the relationship between power, thrust, and velocity. (A8)is the relationship between the temperature and the power and environment, while (A9) indicates that the temperature decreases with increasing altitude. (A10) represents the

relationship between the altitude and speed of an aircraft. Finally, (A11) characterizes the wind acceleration as an uncertain set.

The inner maximization problem in (18) can be transformed into a minimization problem through the strong duality theory, and then merged with the outer minimization problem. After this transformation, the two-stage robust model can be decoupled into a master problem and a subproblem, which can be solved by the C&CG algorithm.

The constraints of the subproblem involve nonlinear functions such as trigonometric functions and bilinear terms, making a direct solution in the solver difficult. To overcome this, certain approximations and transformations can be made. Given that α and γ are small when the plane is flying, sinα and cosβ can be approximated as α and 1-wγ, respectively, where α and β are decision variables and w is a certain constant. As for the bilinear term, the McCormick envelope technique can be utilized to transform it into linear constraints. The McCormick envelope is a relaxation method that ensures both convexity and tight bounds.

III. RELIABILITY AND WEIGHT MODEL OF ELECTRIC POWTRAINS

Reliability allocation optimization for electric powertrains subsystems in electric aircraft requires a functional relationship between weight and reliability ($R_i(m_i)$ in (11)). However, such a relationship is often estimated based on engineering experience without an analytical expression, making it challenging to integrate it directly into optimization models. To address this issue, a mathematical model of weight and reliability for each subsystem is established using Monte Carlo sampling and envelope fitting techniques.

A. Battery pack reliability and weight model

The assessment of battery pack reliability cannot be solely based on its fault state, but rather on the statistical distribution of the health status of multiple battery modules. The first step is to predict the health state of a single battery module, establish a voltage and capacity reliability model, and estimate the overall reliability probability of the battery using the universal generating function (UGF) based on the approach presented in [18]. The mathematical formulation is provided in the Appendix.

Battery reliability comprises voltage reliability and capacity reliability. The battery is connected in series and parallel, and the topology directly affects the voltage reliability of the battery pack. Furthermore, the overall capacity of the battery pack is closely related to the capacity that each battery can provide, and whether it can meet the required power for the voyage is also related to the battery pack's reliability. Therefore, battery pack reliability should encompass both topology reliability and electrical reliability. Battery reliability is the product of topology reliability and capacity reliability, as shown in (19).

$$R_{Bat} = R_{Bat1} \cdot R_{Bat2} \tag{19}$$

While the method presented in [18] ensures the reliability of the voltage, it does not account for situations where the battery pack has insufficient total power to complete the required work, even if only one cell in each parallel branch is in good condition. (20) is presented as a means to calculate the probability of the battery pack completing the task based on an estimation of the capacity of the entire battery pack.

$$J_{\text{bat}} = \frac{P_{\text{cr}} t}{\eta} = \frac{WR}{(L/D)\eta} \tag{20}$$

If the battery pack has completed n cycles of charge and discharge and the remaining capacity is higher than the required capacity for the cruise, it is considered to have a higher probability of successfully completing the task, and thus higher reliability. However, when the remaining capacity is close to the required capacity, the traditional two-state reliability assessment is too strict and may lead to completely different results for similar remaining quantities. To address this, the adjusted sigmoid function is used to replace the traditional two-state step function. The per unit value of the electricity required for a cruise is represented by the abscissa 1, and the adjusted sigmoid function is expressed in (21).

$$R_{Bat2} = \frac{1}{1+e^{-\mathrm{a}(x-1)}} \tag{21}$$

The capacity reliability of the battery pack, denoted as R_{Bat2} can be determined by evaluating the total electric capacity of the battery pack under various topologies and substituting the normalized electric capacity into (21). Subsequently, the overall reliability of the battery pack can be computed using (19).

To obtain the battery weight and reliability data graph, the number of batteries in parallel can be varied and Monte Carlo sampling can be employed for data computation. The functional relationship shown in (22)-(23) can then be derived through curve fitting.

$$R_B(m) = 1 - e^{a_4 m + b_4} \tag{22}$$

$$m_B(R) = c_4 \ln(\frac{1}{1-R}) + d_4 \tag{23}$$

Additionally, considering the non-negligible contribution of other components in the battery pack besides the battery cells, such as the battery management system, the energy density of the battery pack may differ from that of the individual cells. Therefore, a proportional coefficient is introduced to account for this difference, as shown in (24).

$$m_B(R) = \frac{\rho_0}{\rho}(c_4 \ln(\frac{1}{1-R}) + d_4) \tag{24}$$

B. Motor reliability and weight model

At present, there are three types of typically conducting motors utilized in electric aircraft, namely rare earth permanent magnet synchronous motors, DC excited synchronous motors, and induction motors. Among these, the rare earth permanent magnet synchronous motor exhibits a high level of technical maturity, and its power grade and power density can adequately satisfy the requirements of small electric aircraft, making it a popular choice. The common fault modes of permanent magnet brushless synchronous motors are primarily attributed to permanent magnet, winding, and bearing loss. For instance, winding failures can be further classified into turn-to-turn

insulation, phase-to-phase insulation, and inter-slot insulation, with their respective working failure rates as presented in (25). A detailed analysis of component failure rates can be found in [19].

$$\lambda_i = \lambda_b \pi_E \pi_Q \pi_C \pi_K \tag{25}$$

where λ_b is the basic failure rate (10^{-6} per hour), π_E is the environmental coefficient, π_Q is the mass coefficient, π_C is the structure coefficient and π_K is the species coefficient.

Due to the light weight of the permanent magnet, its impact on the weight-reliability relationship of the permanent magnet synchronous motor can be disregarded. Accordingly, the reliability model of the motor is simplified to two series-connected parts, namely, the winding, bearing, and shaft. Although redundancy technology enhances system reliability, it concurrently increases weight and volume. Therefore, the reliability and weight data of the motor with various topologies, including non-redundant, dual-motor, dual-rotor redundant, and single-rotor redundant motor models, are obtained by calculating the reliability and weight of different degrees of redundancy of the motor. Different motor topologies undergo evaluation for their reliability and weight, enabling the construction of motors with lower power levels in parallel to meet specific requirements for total power greater than a certain value and increased reliability upon the occurrence of a fault. Monte Carlo random sampling is employed based on the weight and reliability data of different motors to obtain data diagrams of the reliability and weight of the motor under a specific power level if the motor unit is composed of distinct units. Since certain topologies do not enhance reliability while increasing weight, these points do not constitute valid redundancy in the weight-reliability relationship. Consequently, only the envelope is fitted during function fitting. The upper envelope is determined by utilizing the convhull function to identify the convex hull in the data scatter. Multi-parameters are optimized using a genetic algorithm, achieving the best function fitting of these data points. The resulting function of motor reliability with respect to weight is shown in (26).

$$R_m(m) = 1 - e^{a_1 + b_1 m} \tag{26}$$

A well-designed motor structure exhibits a positive correlation between its reliability and weight. Increasing the unit reliability leads to a higher cost in terms of weight, even though it also leads to increased overall reliability. It should be noted that the weight of a motor is not solely determined by the level of industrial power density, but also by the power grade of the motor.

Based on these assumptions, the function can be applied to motors of any power level and power density, and is expressed in (27).

$$m_m(R, P, w) = f_1(P, w) \cdot (c_1 \cdot \ln(\frac{1}{1-R}) + d_1) \tag{27}$$

where P and w represent the power and power density levels of the motor respectively.

C. Power electronics reliability and weight model

The reliability of power electronics systems, such as DC/DC converters and DC/AC inverters, is a critical aspect of their performance. The relationship between reliability and weight for these systems is analogous to that of motors. For the DC/DC converter, a reliability model is developed that consists of primary and secondary capacitors, a transformer, and two full bridges, with each bridge containing four IGBT modules. Similarly, the reliability of the inverter is mainly determined by the capacitor, IGBT module, and LCL filter, without considering the protection equipment and control circuit. Redundancy technology is applied to these systems at varying degrees, and the overall weight and reliability of the DC/DC converter are computed based on different topologies. Invalid redundant points are eliminated, and envelope fitting of the data points is carried out to obtain data diagrams of the reliability and weight of the DC converter and inverter at a certain power level. The function is then extended to any power level and density in the same way as for motors, as shown in (28)-(29).

$$m_D(R_D, P, w_D) = f_2(P, w_D) \cdot (c_2 \cdot \ln(\frac{1}{1-R_D}) + d_2) \tag{28}$$

$$m_{inv}(R_{inv}, P, w_{inv}) = f_3(P, w_{inv}) \cdot (c_3 \ln(\frac{1}{1-R_{inv}}) + d_3) \tag{29}$$

where m_D and m_{inv} represent the weight of DC/DC converter andinverter; w_D and w_{inv} represent the power density level of DC/DC converter and inverter; R_D and R_{inv} represent their reliability; P represents the rated power required by electric powertrains.

Fig.4 presents the workflow of the proposed reliability allocation model, outlining the steps involved in optimizing the weight-reliability trade-off for the all-electric aircraft powertrain.

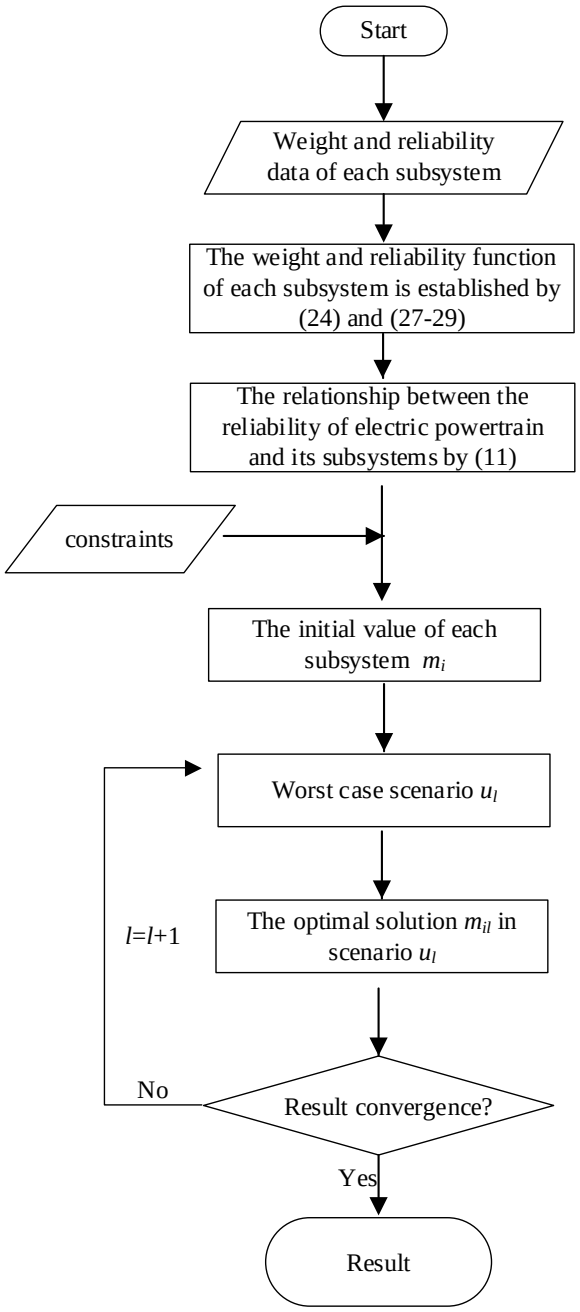

Fig. 4 the workflow of the proposed reliability allocation model

IV. CASE STUDY

First, the functional relationship between the weight and reliability of each subsystem is demonstrated. Based on the fitted functions, the proposed weight-constrained reliability allocation method is applied on the "Spirit of Innovation". We assess three different scenarios: i) one-stage model under rated operating conditions, ii) two-stage model under actual operating conditions and iii) two-stage under different temperature zones to assess the scalability of the proposed model. The results are compared with the baseline design of the "Spirit of Innovation" in terms of weight and reliability at system level and component level.

The "Spirit of Innovation" took its maiden flight in November 2021. Its default parameters are shown in TABLE I, which are used as the baseline in our study.

TABLE I
PARAMETERS OF "SPIRIT OF INNOVATION"

Parameters	Numerical value
Maximum take off weight	1250 kg
Batteries*	18650
Voyage	180 miles
Battery capacity	3 Ah
Battery voltage	3.7 V
Battery weight	48 g
Battery pack	18*10p36s,72kWh/474kg
Motor	400 kW/200 kg
Inverter	400 kW/75 kg
DC/DC	400 kW/90 kg
Wing area	18 m^2
Lift coefficient*	0.35
Drag coefficient*	0.032
Maximum thrust*	8000 N

A. Functional relationship between subsystem weight and reliability

The reliability and weight data of each part of a 133kW, 67kg permanent magnet synchronous motor are shown in TABLE II(with a rated temperature of 120℃ and a working duration of 10,000 hours).

TABLE II
RELIABILITY ASSESSMENT OF A 133KW, 67KG PERMANENT MAGNET SYNCHRONOUS MOTOR

Parameters	Shaft and bearing	winding	Others (magnetic steel, iron core casing, etc.)
failure rate/10^{-6}	0.1630	0.3408	<0.01
weight/kg	7.5	12.5	47

Analysis of this table reveals that that for the permanent magnet brushless motor, the winding failure rate is the highest, but the weight is relatively small. Consequently, redundancy in this part has the most significant impact on improving reliability per unit weight. On the other hand, the failure rates of parts such as magnetic steel and iron core are very low, and they are also heavy, so redundancy in these parts does not have much effect on improving reliability. Based on this analysis, we carried out different degrees of redundancy for the motor and observed the changes in its reliability, as depicted in Fig.4.

**The parameters of the battery pack are estimated based on the voltage and capacity of each battery pack, while the values of the inverter and lift-to-drag ratio are the same as those of a similar electric aircraft.*

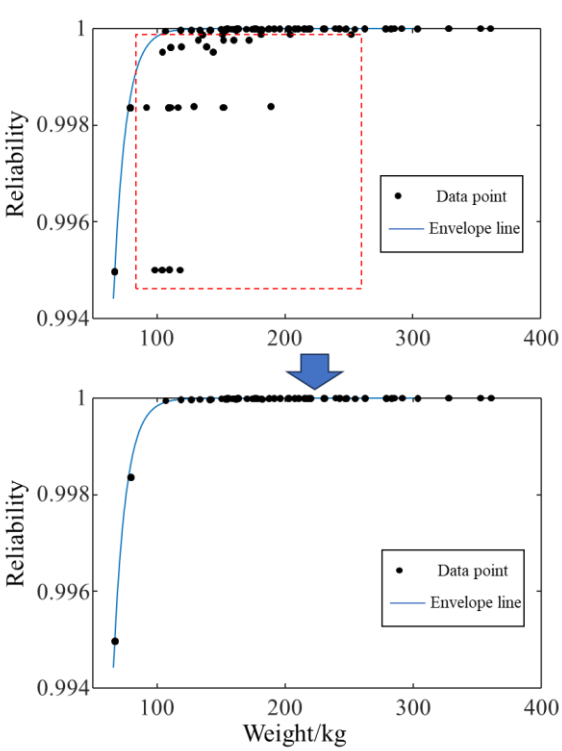

Fig. 4 Motor reliability and weight data graph

Within the weight range of 70-90 kg, the motor's reliability increases sharply, primarily due to redundancy in the motor winding. Around 100 kg, the improvement in reliability reaches saturation, and further redundancy does not significantly augment the motor's reliability. Certain points in the figure only add weight to the motor without markedly enhancing its reliability; these are deemed ineffective redundancy and are encircled in red in Fig.4 to distinguish them from the rest of the data. During the fitting of the reliability and weight function, these points are excluded.

Feeding the simulated data into (27), we can get the specific form of the relationship between motor weight and reliability as shown in (A19) in appendix. In a similar way, the weight-reliability function of converter and battery are expressed in (A19) and (A20).

B. Reliability allocation considering rate working conditions

Under rated operation condition (specifically, the motor is at 120℃, the power electronics are at 85℃, and the battery is at 25℃), the reliability of subsystems are calculated. After each component has operated for a certain duration (2000 hours for the battery pack and 10,000 hours for the other components), reliability is optimized with the objective of maximum reliability, using the Gurobi solver. The original parameter and optimal reliability allocation of the aircraft at the rated temperature are detailed in TABLE III.

TABLE III
RELIABILITY ALLOCATION OF "SPIRIT OF INNOVATION" AT RATED WORKING CONDITIONS

Parameters	Baselined weight/ **optimized weight**(kg)	Baselined reliability/ **optimized reliability**
Battery	474/**465.56(↓)**	0.9967/**0.9948(↓)**
DC/DC	90/**103.44(↑)**	0.9834/**0.9877(↑)**
Inverter	75/**90.00(↑)**	0.9607/**0.9869(↑)**
Motor	200/**180.00(↓)**	0.9951/**0.9926(↓)**
System	839/839(-)	0.9370/**0.9626(↑)**

After optimization, it can be seen that the reliability of the aircraft has increased from the original value of 0.9370 to 0.9626, while the weight of the system remains the same. This is because the weight cost of improving battery reliability is relatively high. Therefore, consideration may be given to reducing the weight of the battery through secondary distribution. In addition, increasing the IGBT redundancy of the inverter and DC/DC converter can improve system reliability at a small weight cost. The weight reduction of the motor system can be considered from the perspective of distributed systems by changing the original three-engine system to a two-engine system.

C. Reliability allocation considering actual working conditions

Using the proposed model, a worst-case wind speed scenario can be generated after determining an initial value in the first stage, as depicted in Fig.5. Through iterative optimization in the two stages, an optimal reliability allocation with a certain degree of robustness under actual operating conditions can be obtained.

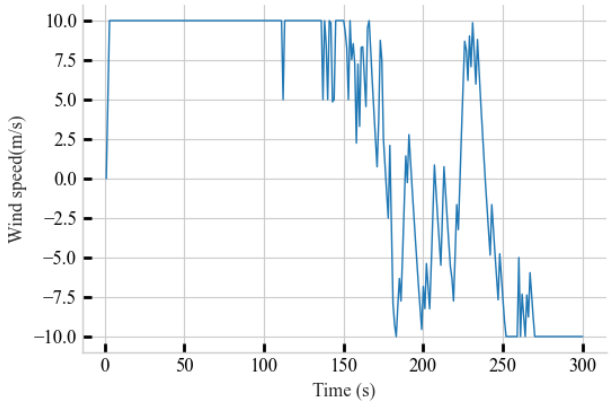

Fig. 5 Wind speed set in the worst scenario based on initial parameter

In Fig.5, wind speed values greater than zero indicate a tailwind, while values less than zero indicate a headwind. The figure reveals that the worst-case scenario occurs when the aircraft takes off with a prolonged period of tailwind, which can adversely affect its flight. In the worst-case scenario, the temperature variation curves of various aircraft components are shown in Fig. 6, reflecting adjustments made to the propulsion power.

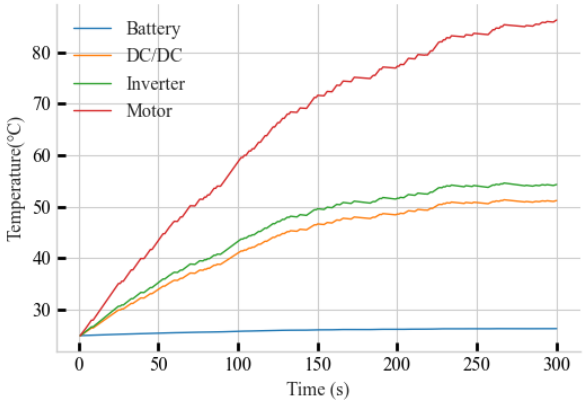

Fig. 6 Actual temperature curve of each subsystem after optimization

It can be observed that the temperature of all components increases continuously after takeoff, with the highest temperature being recorded in the motor and the lowest temperature in the battery. The comparison between the results of reliability allocation under the consideration of only standard cases and under the consideration of two-stage robustness is shown in TABLE V. The reason for the higher reliability compared to standard conditions is that in actual operation, small aircraft may rarely reach the rated temperature of components such as motors.

TABLE V
RELIABILITY PARAMETERS OF TWO METHOD OF "SPIRIT OF INNOVATION"

Parameters	Optimal allocation in rated situation / **two-stage optimal allocation** (kg)	Reliability in actual situation
Battery	465.56/**472.41(↑)**	-
DC/DC	103.44/**96.69(↓)**	-
Inverter	90.00/**90.00(-)**	-
Motor	180.00/**180.00(-)**	-
System	839/839	0.9865/**0.9870**

As shown in TABLE V, it can be ovserved that using the two-stage optimization method for aircraft reliability allocation design results in better reliability performance in actual working conditions and is more in line with actual application scenarios.

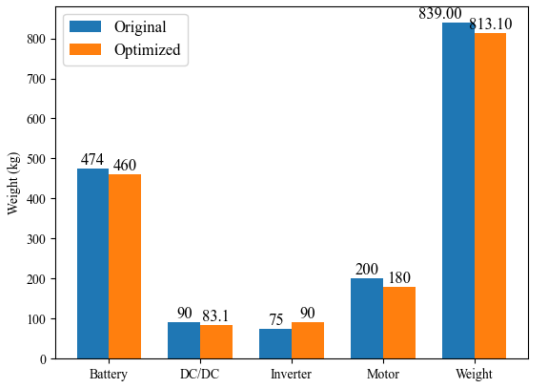

Fig. 7 Comparison of Original and Optimized Aircraft Parameters

In addition, we incorporated the baseline weight parameters of the aircraft into the model and found that the aircraft's reliability under the worst wind speed condition can reach a maximum of 0.9786. By using the proposed reliability allocation model and changing the total weight constraint of the system, a reliability level of 0.9786 can be achieved with only 813.1kg as shown in Fig.7. In other words, if the actual reliability of the aircraft in practical operating conditions remains unchanged, a weight reduction of 25.9 kg can be achieved by a reasonable allocation of reliability. In general, the reliability of other components can be appropriately reduced while improving the reliability of the inverter. This can reduce weight without compromising the overall system reliability.

D.Reliability allocation considering different temperature zones

The temperature range of an aircraft's environment can vary significantly depending on latitude, leading to substantial differences in environmental temperature at identical flight altitudes. Consequently, this section considers the reliability allocation of the aircraft under different temperature ranges, aiming to provide reliability allocation references for aircraft at different latitudes.

Two temperature zones were selected for analysis: Region 1, characterized by an average ground temperature of 10℃ throughout the year, and Region 2, with an average ground temperature of 20℃. Reliability two-stage allocation optimization was conducted under these conditions, and the results are depicted in Fig.8.

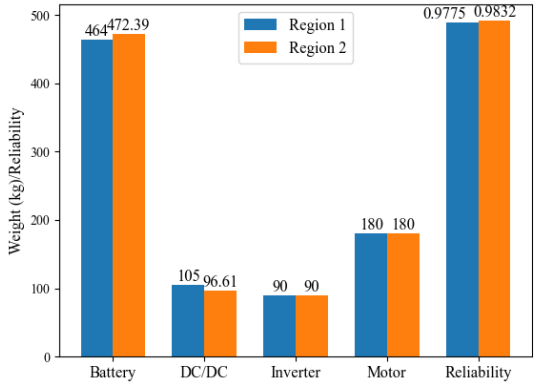

Fig. 8 Comparison of Optimized Aircraft Parameters in Different Region

As illustrated in Fig.8, the optimization outcomes differ between the two temperature zones. Specifically, the overall reliability of Region 1 is lower than that of Region 2. This discrepancy is attributed to the lower environmental temperature in Region 1, which significantly diminishes the battery's reliability, thereby impacting the overall system reliability. In higher latitude regions (such as Region 1), the proposed method exhibits a tendency to allocate reliability to power electronics equipment, as these components can achieve enhanced reliability with a smaller weight penalty.

V.CONCLUSION

In this paper, we proposed a two-stage reliability allocation method for electric aircraft powertrain design that takes into account temperature and actual operating conditions. Our approach considers the actual operating temperature of

components, which is closely related to environmental temperature and component weight. We applied our approach to a case study using the " Spirit of Innovation " electric aircraft and demonstrated its effectiveness in improving the overall reliability and reducing weight compared to traditional methods that assume constant temperature values.

Our results show that the optimal reliability allocation varies with different temperature zones, highlighting the importance of considering actual operating conditions. The proposed two-stage model provides a more accurate and robust approach for reliability allocation in electric aircraft powertrain design. The method is also scalable and can be applied to different latitude zones. The findings of this study have practical implications for designing electric aircraft powertrains with improved reliability and reduced weight.

Overall, the proposed approach provides a more comprehensive and accurate methodology for allocating reliability and optimizing weight in electric aircraft powertrain design. It represents a significant step forward in enhancing the reliability and performance of electric aircraft and provides a foundation for future research in this area.

APPENDIX

$$M(\vec{V}_j+\vec{V}_{wj}.\cos\gamma_j)=TN_j\cos\alpha-D_j-Mg\sin\gamma_j \quad \text{(A1)}$$

$$M(V_j+V_{w_j})\dot{\gamma}_j=TN_j\sin\alpha_j+L_j-Mg\cos\gamma_j \quad \text{(A2)}$$

$$V_j=V_{j-1}+\vec{V}_{j-1} \quad \text{(A3)}$$

$$V_{w_j}=V_{w_{j-1}}+\vec{V}_{w_{j-1}} \quad \text{(A4)}$$

$$L_j=\frac{1}{2}\rho(V_j+V_{wj})^2S\cos\gamma_jC_L \quad \text{(A5)}$$

$$D_j=\frac{1}{2}\rho(V_j+V_{wj})^2S\cos\gamma_jC_D \quad \text{(A6)}$$

$$P_j=T_jV_j \quad \text{(A7)}$$

$$C_im_i(T_{i,j}-T_{i,j-1})=P_{j-1}l_i-A_i(T_{i,j-1}-Th_{j-1}) \quad \text{(A8)}$$

$$Th_j=25-0.006h_j \quad \text{(A9)}$$

$$h_j=h_{j-1}+V_{j-1}\sin\gamma_{j-1} \quad \text{(A10)}$$

$$\vec{V}_{wj}\in U \quad \text{(A11)}$$

where variable V_j is the aircraft speed at time instant j, V_{wj} is the wind speed at time instant j and c are constant series vectors. The available (A12) predicts the SOH state of the battery.

$$\mathrm{SOH}_i=1-\sum_{i=1}^{A}\frac{|P_{B,i}|}{2\times N_{equ,i}(|P_{B,i}|)\times Q_{ini}}\times t_i \quad \text{(A12)}$$

UGF of the battery can be expressed as Formula (4).

$$G_{SOH}(z)=\sum_{i=1}^{Y}p_lz^{e_i} \quad \text{(A13)}$$

After determining the UGF representation of a single battery, the combined UGF between battery i and j can be obtained through Formula (A14), which can be extended to the UGF representation of the whole battery pack, thus obtaining the probability set of each state of the battery pack.

$$\otimes\left(G_{SOH,i}(z),G_{SOH,j}(z)\right)=\sum_{i=1}^{Y}\sum_{j=1}^{Y}p_ip_jz^{f(e_i,e_j)} \quad \text{(A14)}$$

where $\otimes$ is the combination operator, representing the UGF combined operation of two batteries; Every possible value of f corresponds to a combination of e_i and e_j, and its calculation method can be determined by (A15).

$$f(e_i,e_j)=\begin{cases}\max(e_i,e_j), & in\ \ parallel\\ \min(e_i,e_j), & in\ \ series\end{cases} \quad \text{(A15)}$$

When the battery topology is known, such as the parallel connection of a battery module, the UGF of this group of parallel branches can be obtained from Formula (A16). When the battery pack is connected in series by group b branches, the UGF of the battery pack can be obtained from (A17).

$$\begin{aligned}G_{para}(z)&=\otimes\left(G_{SOH,1}(z),\ldots,G_{SOH,a}(z)\right)\\&=\sum_{s=1}^{a}p_sz^{e_s}\end{aligned} \quad \text{(A16)}$$

$$\begin{aligned}G_{battery}(z)&=\otimes\left(G_{para,1}(z),\ldots,G_{para,b}(z)\right)\\&=\sum_{l=1}^{b}p_lz^{h_l}\end{aligned} \quad \text{(A17)}$$

where e_s is the SOH level after parallel operation, and p_s is its corresponding probability. h_l is the SOH level of the entire battery pack, and p_l is its corresponding probability.

If threshold α is specified, the voltage reliability of the battery pack is shown in (A18).

$$R_{Bat1}=pr\{h_l\ge\alpha\}=\sum_{h_l\ge\alpha}p_l \quad \text{(A18)}$$

$$\begin{aligned}\begin{bmatrix}m_m(P,R_m)\\m_D(P,R_D)\\m_{inv}(P,R_{inv})\end{bmatrix}^T&=\begin{bmatrix}-4.589\times10^{-6} & 8.381\times10^{-3} & -0.0381\\-6.855\times10^{-6} & 0.0782 & -0.0932\\-1.060\times10^{-5} & 0.0072 & -0.0426\end{bmatrix}\cdot\\&\begin{bmatrix}P^2\\P\\1\end{bmatrix}\cdot\begin{bmatrix}16.74\ln(\frac{1}{1-R_m})-22.25\\14.82\ln(\frac{1}{1-R_D})-30.71\\4.95\ln(\frac{1}{1-R_{inv}})+8.9911\end{bmatrix}^T\end{aligned} \quad \text{(A19)}$$

$$m_B(R_B)=-28.1694\ln(\frac{1}{1-R_B})+559.1617 \quad \text{(A20)}$$

REFERENCES

[1] H.Jun, et al. ,"New energy electric aircraft development and challenges,". *Acta Aeronautica et Astronautica Sinica*, vol.37, no. 3, pp. 57-68,

Feb.2016.
[2] B. Krueger, G. Filomeno, A. Golle, D. Dennin and P. Tenberge, “Unified Mode-Based Description of Arbitrary Hybrid and Electric Powertrain Topologies,” *IEEE Trans. Veh. Technol.*, vol. 71, no. 2, pp. 1293-1306, Feb. 2022.
[3] C. Yi, H. Hofmann and B. I. Epureanu, “Energy Efficient Platooning of Connected Electrified Vehicles Enabled by a Mixed Hybrid Electric Powertrain Architecture,” *IEEE trans. Intell. Transp. Syst.*, vol. 23, no. 11, pp. 20383-20397, Nov. 2022.
[4] P. Ghimire, M. Zadeh, J. Thorstensen and E. Pedersen, “Data-Driven Efficiency Modeling and Analysis of All-Electric Ship Powertrain: A Comparison of Power System Architectures,” *IEEE Trans. Transp. Electrification*, vol. 8, no. 2, pp. 1930-1943, June 2022.
[5] C. A. Luongo et al., “Next Generation More-Electric Aircraft: A Potential Application for HTS Superconductors,” *IEEE Trans. Appl. Supercond.*, vol. 19, no. 3, pp. 1055-1068, June 2009.
[6] Z.Dong et al., “Research on High Power Density SiC Motor Drive Controller”. *Proceedings of the CSEE*, vol. 39, no. 19, pp. 5624-5634+5890. Oct. 2019.
[7] W. Li, S. Pai, M. Kwok and J. Sun, “Determining rational redundancy of 500-kV reactors in transmission systems using a probability-based economic analysis approach: BCTC's practice,” *IEEE Trans. Power Syst.*, vol. 19, no. 1, pp. 325-329, Feb. 2004.
[8] H. Pham, “Optimal cost-effective design of triple-modular-redundancy-with-spares systems,” *IEEE Trans. Rel.*, vol. 42, no. 3, pp. 369-374, Sept. 1993.
[9] Y. Cao, S. Liu, Z. Fang and W. Dong, “Reliability Improvement Allocation Method Considering Common Cause Failures,” *IEEE Trans on Rel.*, vol. 69, no. 2, pp. 571-580, June 2020.
[10] S. Si, M. Liu, Z. Jiang, T. Jin and Z. Cai, “System Reliability Allocation and Optimization Based on Generalized Birnbaum Importance Measure,” *IEEE Trans on Rel.*, vol. 68, no. 3, pp. 831-843, Sept. 2019.
[11] W. Kuo, V.R. Prasad,F. A. Tillman, and C.L.Hwang,Optimal Relia-bility Design: Cambridge University Press, 2001.
[12] B. Hu, K. Xie and H. -M. Tai, “Optimal Reliability Allocation of ±800 kV Ultra HVDC Transmission Systems,” *IEEE Trans on Power Del.*, vol. 33, no. 3, pp. 1174-1184, June 2018.
[13] Z. -J. Liu and Q. -F. Song, “Reliability allocation multi-objective optimization for products under warranty,” in 2012 International Conference on Quality, Reliability, Risk, Maintenance, and Safety Engineering, Chengdu, China, 2012, pp. 423-426.
[14] M. Catelani, L. Ciani, G. Patrizi and M. Venzi, “Reliability Allocation Procedures in Complex Redundant Systems,” *IEEE Syst. J.*, vol. 12, no. 2, pp. 1182-1192, June 2018.
[15] L. Shen, Y. Zhang, Q. Zhao, C. Chen, K. Song, B. Song, “A Reliability Allocation Methodology for Mechanical Systems With Motion Mechanisms,” *IEEE Syst. J.*, vol.16, no.4, pp.5596-5607, Dec. 2022.
[16] F. Chen et al., “Reliability allocation for CNC turrets based on fuzzy comprehensive evaluation,” in 2016 11th International Conference on Reliability, Maintainability and Safety (ICRMS), Hangzhou, China, 2016, pp. 1-6.
[17] X. Shang, W. Han, C. Li， W. Dong, “ A new approach to aircraft system reliability assignment,” *Ordnance Industry Automation*, vol. 29, no. 12, pp. 16-19, Dec. 2010.
[18] M. Liu, W. Li, C. Wang, M. P. Polis, L. Y. Wang and J. Li, “Reliability Evaluation of Large Scale Battery Energy Storage Systems,” *IEEE Trans. Smart Grid*, vol. 8, no. 6, pp. 2733-2743, Nov. 2017.
[19] MIL-HDBK-338B: *Electronic Reliability Design Handbook*, Dept. Defence, Washington, DC, USA, Oct. 1988.